IOPscience iopscience.iop.org

Home Search Collections Journals About Contact us My IOPscience

Ordering and magnetic hyperfine fields in $Pt_3Mn_{0.9}Fe_{0.1}$ studied by Mossbauer spectroscopy

This article has been downloaded from IOPscience. Please scroll down to see the full text article.

1991 J. Phys.: Condens. Matter 3 5469

(http://iopscience.iop.org/0953-8984/3/29/002)

View the table of contents for this issue, or go to the journal homepage for more

Download details:
IP Address: 171.66.16.147
The article was downloaded on 11/05/2010 at 12:22

Please note that terms and conditions apply.

J. Phys.: Condens. Matter 3 (1991) 5469–5478. Printed in the UK

Ordering and magnetic hyperfine fields in $Pt_3Mn_{0.9}Fe_{0.1}$ studied by Mössbauer spectroscopy

K Szymański†, L Dobrzyński†, E Gerkema‡ and A M van der Kraan‡
† Physics Faculty, Warsaw University Branch, Białystok, Poland
‡ Interfacultair Reactor Instituut, Delft, The Netherlands

Received 3 May 1990, in final form 3 January 1991

Abstract. The influence of structural defects on the magnetic properties of $Pt_3Mn_{0.9}Fe_{0.1}$ are studied by means of Mössbauer spectroscopy. The magnetic hyperfine field distribution shows that the sample exhibits an inhomogeneous magnetization distribution. The cold work introduces a number of antiphase boundaries dividing the sample into subvolumes with the linear dimensions of 30–100 Å. The magnetization of these subvolumes performs a superparamagnetic-like relaxation. The origin of relaxation is discussed.

1. Introduction

$Pt_3Mn_xFe_{1-x}$ alloys crystallize in a face centred cubic structure (Pickart and Nathans 1962, Bacon and Crangle 1963, Shreiner *et al* 1985) which upon ordering changes to the so-called $L1_2$ superstructure. The $L1_2$ superstructure is easily achieved after quenching from the melt (Stamm and Wassermann 1986) or from the disordered state after annealing at relatively low temperatures in short times (Sidorov and Dubinin 1967).

At low temperatures, ordered Pt_3Mn is ferromagnetic, while Pt_3Fe is antiferromagnetic. A mixture of both systems indicates a complex magnetic behaviour which was first interpreted as a canted non-collinear spin structure (Vokhmyanin *et al* 1980). However, the low-temperature properties of $Pt_3Mn_xFe_{1-x}$ were also explained within the framework of the re-entrant spin-glass model (Shreiner *et al* 1985). At higher temperatures a superparamagnetic phase is observed.

The magnetic properties of Pt_3Mn and Pt_3Fe are very sensitive to structural disorder. After plastic deformation the alloys change their magnetic order and become, at room temperature, paramagnetic and ferromagnetic, respectively (Crangle 1959, Bacon and Crangle 1963, Shreiner *et al* 1985). It was suggested (Ikeda and Takahashi 1984) that magnetic changes are caused by slip-induced dislocations. Within the antiphase boundary (APB) extending between a pair of dislocations, atoms are changing their local environments and induce changes in local magnetic order.

It should be remembered that defects such as dislocations and APBs can exist in long-range ordered structures and will then be undetectable in diffraction experiments. However, the Mössbauer effect will be helpful in detecting the influence of this kind of defect on the magnetic structure. The observed Mössbauer spectra of Pt–Fe–Mn alloys show an inhomogeneity in the magnetic hyperfine field distribution (MHFD): a paramagnetic-like absorption line coexisting with Zeeman sextets. This effect becomes

0953-8984/91/295469 + 10 $03.50 © 1991 IOP Publishing Ltd

particularly clear when the temperature is approaching the magnetic transition temperature T_c (Segnan 1967, Vinokurova *et al* 1969). The behaviour of some of the systems can be explained by relaxation effects (Szymański and Dobrzyński 1990).

2. Experimental details

2.1. Sample preparation

$Pt_3Mn_{0.9}Fe_{0.1}$ was prepared by repeated (a few times) melting of a mixture of 99.8% Pt, 99.998% Mn and spectrally pure Fe enriched in the Mössbauer isotope ^{57}Fe, in an arc furnace under a high-purity argon atmosphere. The mass losses did not exceed 0.21%.

The sample used for conversion electron Mössbauer spectroscopy (CEMS) consisted of grains with linear dimensions of about 0.5 mm. Such a sample should be well ordered (according to Shreiner *et al* (1985) 'no special annealing treatments are necessary to install the ordering').

In order to prepare the samples for Mössbauer spectra measurements in transmission geometry, they were homogenized in vacuum in a quartz tube (1300 K for 12 h) and powdered in an agalite ball mill. The powder obtained was then mixed with Al_2O_3 and pressed into pellets. To achieve the $L1_2$ type of ordering the pellets were annealed and the details will be described in section 3.1. The evaporation of manganese is prevented by annealing the samples together with manganese powder in evacuated quartz tubes.

Mössbauer measurements at various temperatures were carried out on two different samples. Thermal treatment of the first sample (sample I) is described in section 3.1. In the final stage it was annealed at 720 K for 24 h and cooled with the furnace. This sample turned out to be slightly disordered. The second sample (sample II) was annealed at 1060 K for 6 h and cooled at a rate of 2.9 K h^{-1}; it turned out to be well ordered.

2.2. Apparatus

The Mössbauer spectra were recorded in a constant-acceleration mode. The measurements at room temperature and above were performed in the laboratory of Warsaw University, Białystok, using ^{57}Co in a Cr matrix at room temperature as the source. The measurements below room temperature were carried out at the Intefacultair Reactor Instituut, Delft, with a ^{57}Co in Rh source. The isomer shift (IS) is given relative to α-Fe as the absorber for both sources.

The furnace employed consists of two coaxial cylindrical heaters which ensure that the sample has a low temperature gradient. The temperature was measured and controlled by a chromel–alumel thermocouple. Every Mössbauer spectrum was recorded for 1–3 d and during that period the temperature was stabilized in the range 0.1–0.7 K.

3. Results

3.1. Results of the thermal treatment

After quenching from melt, the as-cast bulk material acquires the $L1_2$ superstructure (Shreiner *et al* 1985). Also, Shreiner *et al* conclude from the x-ray diffraction, microprobe analysis and magnetization measurements that alloys of this kind are homogeneous on

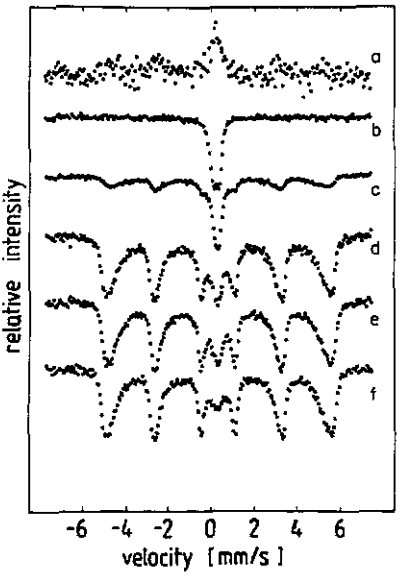

Figure 1. Room-temperature Mössbauer spectra of $Pt_3Mn_{0.9}Fe_{0.1}$: spectrum a, bulk sample just after melting and crushing to grains of about 0.5 mm, measured with CEMS; spectra b–f, transmission spectra of sample I after consecutive stages of thermomechanical treatments (spectrum b, after powdering; spectrum c, after annealing at 570 K for 63 h; spectrum d, after annealing at 670 K for 24 h; spectrum e, after annealing at 670 K for 29 h; spectrum f, after annealing at 720 K for 24 h).

the macroscopic scale and exhibit long-range order. The conversion electron spectrum of the bulk sample which was measured by us and is shown in figure 1, spectrum a, reveals the features of the ordering on the microscopic scale. It is clear from this figure that the Zeeman sextet coexists with a paramagnetic-like peak; so the magnetic ordering cannot be complete.

The Mössbauer spectrum of the disordered alloy (after powdering) at room temperature consists of two absorption lines at a distance of about 0.27 mm s^{-1} (figure 1, spectrum b) which was determined in a separate experiment. Figure 1, spectra c–f, shows the room-temperature Mössbauer spectra of $Pt_3Mn_{0.9}Fe_{0.1}$ after various stages of annealing. It is evident that the intensity of the paramagnetic-like line decreases with increasing annealing temperature and attains some characteristic value for a given annealing temperature. Longer annealing times at the same temperature do not change the relative intensity of the line (figure 1, spectra d and e). The annealing process has been terminated at 1060 K when the room-temperature spectrum contained a negligible content of the paramagnetic line. Spectra of the samples I and II, measured at different temperatures are shown in figures 2(*a*) and 4, respectively.

3.2. Spectra fitting with MHFD

From the measured spectra the MHFD has been calculated using the method of Le Caer and Dubois (1979). Because the spectra are nearly symmetric a zero quadrupole splitting and a constant IS were assumed in the analysis. The relative intensity of spectral lines 2 and 5 has been obtained from the spectra measured at 4.3 K and was kept constant for all other temperatures.

Two different MHFDs were calculated for each spectrum. In the first case the magnetic hyperfine field (MHF) was assumed to extend from zero to an H_{max}-value. H_{max} was chosen as the value at which $P(H_{max})$ was equal to zero. From the analysis of the spectra it follows that the MHFD for both samples extends to very low values even at 4.3 K (figure

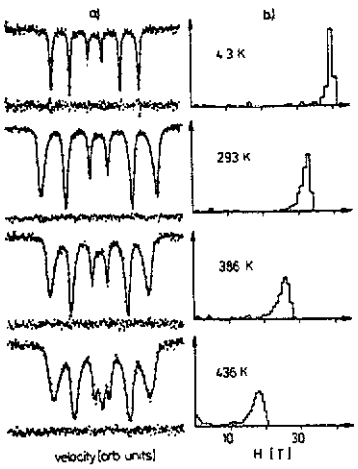

Figure 2. (*a*) Mössbauer spectra of sample I of $Pt_3Mn_{0.9}Fe_{0.1}$, measured at various temperatures and (*b*) the MHFD calculated in partition from zero to a H_{max}-value. The differences between the experimental and calculated points are shown below the spectra. Note that the velocity scales used are different for various spectra.

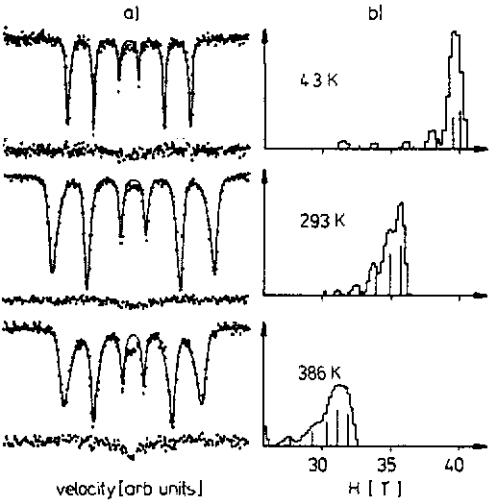

Figure 3. (*a*) Mössbauer spectra of sample I of $Pt_3Mn_{0.9}Fe_{0.1}$, measured at various temperatures and (*b*) the MHFD calculated in only the high-field region. Differences between the experimental points and the theoretical line are shown below the spectra. In the $P(H)$ histograms the values and relative intensities of the MHF obtained from the fitting procedure are indicated.

2(*b*)). Because of the limited number steps in the fitted MHFD, details in the spectra are not well reproduced and particularly in lines 1 and 6 a discrepancy is seen (figure 2(*a*)).

In the second case the details of the shape of the MHFD at high fields were studied. The distributions presented in figure 3(*b*) reproduce well the shape of spectral lines 1 and 6. However, in that case, the discrepancies appear in the central part of the spectra (figure 3(*a*)) which correspond to the low-intensity tail in the $P(H)$ distribution at low temperatures (figure 2(*b*)).

From the analysis of the spectra it followed that the peaks observed in the MHFD become broader with increasing temperature (figure 3(*b*)).

It was checked that the shape of the MHFD was independent of the number of field steps used as well as of the value of the smoothing parameter (Le Caer and Dubois 1979).

3.3. Fitting with a set of Zeeman sextets

Discrete values of the MHF and other microscopical parameters were determined by fitting the spectra with a set of Zeeman sextets and one Lorentzian line. Usually five sextets were needed to obtain a good fit. However, when the spectra were accumulated with somewhat worse statistics, only three sextets were used. It was verified that by taking a fewer number of sextets the parameters of remaining sextets did not change by more than the statistical errors.

In order to test whether the IS is dependent on the value of MHF the spectra were fitted in three different ways. In the first approach the IS was assumed to be the same for all sextets used. In the second fitting method a linear correlation between the IS and the

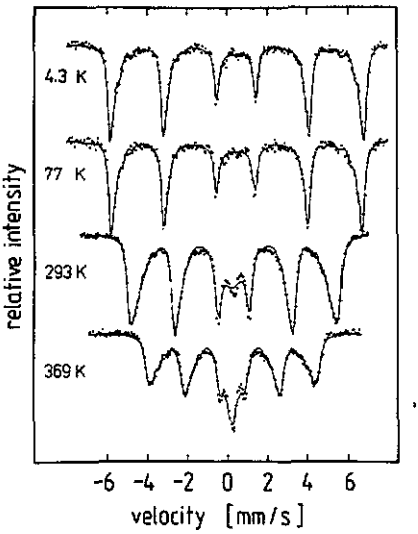

Figure 4. Mössbauer spectra of sample II of $Pt_3Mn_{0.9}Fe_{0.1}$ measured at different temperatures fitted by a set of Zeeman sextets and a single Lorentzian line.

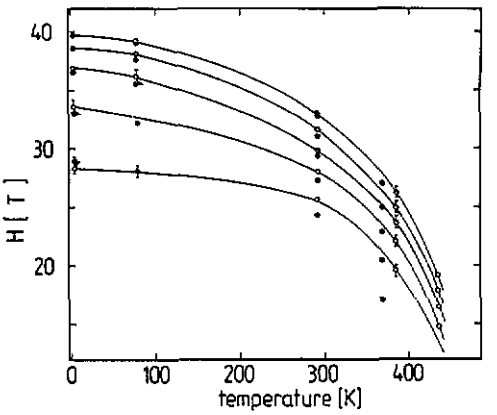

Figure 5. Different values of the MHF versus temperature obtained from the fitting procedure using discrete MHFs: ●, sample I; ○, sample II; ——, lines drawn to guide the eye.

MHF was introduced, while in the third method the IS was allowed to vary by a constant value Δ(IS) for different sextets.

There were not more than 16 independent microscopical parameters in the fitting procedure: the relative intensity and MHF for each sextet, the mean value of the IS, the common linewidth, the intensity ratio of lines 2 to 5, and the parameter describing the changes in the IS versus the MHF for the set of Zeeman sextets. The last three parameters were the linewidth IS and relative intensity for the single Lorentzian line.

Some of the fitting results are displayed in figure 4. The MHFs and their intensities are schematically shown in figure 3 and it follows that the positions of the peaks of the MHFD coincide with the discrete fields. Although slightly smaller values of the MHF are observed for sample I, the fields for both samples exhibit similar temperature behaviours (figure 5).

As mentioned above, also the possibility of having a correlation between H_{eff} and IS is considered. By introducing a linear correlation between H_{eff} and IS as a free parameter, χ^2 is reduced by 1–2% when $\mathrm{d(IS)}/\mathrm{d}H_{\text{eff}} = 0.012 \pm 0.005\ \text{mm s}^{-1}\,\text{T}^{-1}$. Assuming a constant increment Δ(IS) of IS equal to $0.0010 \pm 0.0005\ \text{mm s}^{-1}$ for consecutive sextets, a similar reduction in χ^2 is found and so it is impossible to distinguish between these two assumptions. This turned out to be true for sample I as well as for sample II.

In figure 6(*a*) the values of IS of the paramagnetic-like line and of the Zeeman sextets are displayed as a function of the temperature. The second-order Doppler shift which causes a decrease in the IS of the Zeeman sextets with increasing temperature is observed for both samples. The difference in IS between the paramagnetic-like line and the Zeeman sextets is about $0.1\ \text{mm s}^{-1}$ at low temperatures but vanishes with increasing temperature. This effect is particularly clear for the slightly disordered sample I, for which the central line is more pronounced.

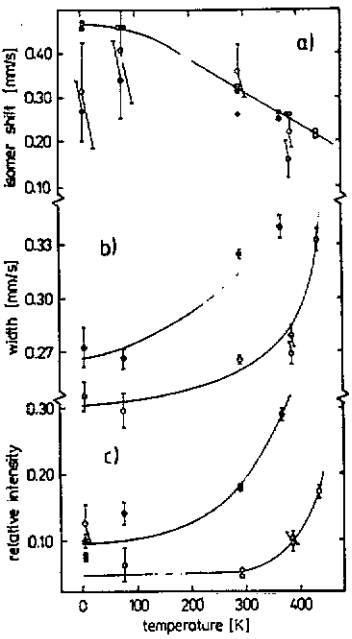

Figure 6. (*a*) Average value of the IS of the Zeeman sextets (□, ■) and of the low-field component fitted by a single Lorentzian line (○, ●); (*b*) half-width of the Lorentzian lines in the Zeeman sextets; (*c*) relative intensity of the low-field component fitted by a single Lorentzian line (○, ●) and obtained from the MHFD (□, ■): ■, ●, sample I; □, ○, sample II; ——, lines drawn to guide the eye.

With increasing temperature the linewidths of the Zeeman sextets become larger (figure 6(*b*)). At the lowest temperatures these linewidths for sample II are only about 20% greater than those observed for thin iron foil.

An important feature of the measured system is the presence of the paramagnetic-like line in the spectrum. The intensity of the line seems to be constant at low temperatures but to increase with increasing T at higher temperatures (figure 6(*c*)). Moreover, at higher temperatures there exist systematic discrepancies between the fitted Lorentzian curve and the experimental data points (figure 4). This means that the shape of the central line is not well described by the Lorentzian curve and hence its identification as the paramagnetic line may be questioned. Its half-width is about 0.8–1.5 mm s^{-1}. The intensity of the paramagnetic-like line agrees well with the relative content of the low-field part in the MHFD (figure 6(*c*)).

4. Discussion

4.1. The process of structural ordering

As was shown by Elkholy and Nagy (1962), annealing in Cu_3Au, the prototype structure of $Pt_3Mn_xFe_{1-x}$, is connected with two processes: changes in crystal domain sizes and ordering within these domains. The latter process was found to be strictly reversible, while the domain sizes irreversibly increase at increasing temperature. In $Pt_3Mn_xFe_{1-x}$ with the $L1_2$ type of structure the slip-induced APB in the [111] plane contains pairs of d atoms which are first-nearest neighbours (Ikeda and Takahashi 1984). It is known that the Mn atom which occupies a Pt site in Pt_3Mn interacts antiferromagnetically with its nearest-neighbour Mn atoms (Menzinger *et al* 1972). When the sample is crushed, a

large density of dislocations and APBs appears. Such APBs therefore affect the ferromagnetic order seen as a strong reduction in the magnetization of Pt_3Mn after cold work (Shreiner *et al* 1985).

The same phenomenon seems to be observed here. The fast (comparable with heat treatment time) positional ordering process leading to the $L1_2$ superstructure, as seen in diffraction experiments (Shreiner *et al* (1985) and references therein), is followed by magnetic ordering within the crystal domains. At the same time, the slip-induced APBs can still exist. As can be inferred from the Mössbauer spectra, longer annealing times at a given temperature do not cause observable changes in the magnetic order (figure 1, spectrum d and e). Hence, the process of ordering at a given temperature seems to saturate easily. It is most probable that the APBs are responsible for the magnetic disorder seen as the paramagnetic-like line in our Mössbauer spectra (figure 1). This point will be discussed in greater detail below.

From our studies it follows that the formation of the $L1_2$ superstructure is not sufficient for attaining a magnetic homogeneity. The defects appearing during alloy crystallization after its quenching from the melt highly perturb the magnetic order (figure 1, spectrum a), and the statement of Shreiner *et al* (1985), cited in section 2.1, should be treated with some caution.

4.2. Low-temperature behaviour

In the well ordered $Pt_3Mn_xFe_{1-x}$ alloy (sample II) the first coordination shell of a 3d atom should be filled by 12 Pt atoms and the second shell by six 3d atoms. So, the observed MHFD will primarily be due to a different number of Mn and Fe atoms in the second coordination shell. From the set of fitted hyperfine fields the value of the MHF at an iron site surrounded exclusively by Fe atoms (as in Pt_3Fe) has been estimated. The extrapolated values are 25 ± 2 T at 4.3 K and 24 ± 2 T at 77 K. They correspond reasonably to the published values for iron–platinum alloys: 27.8 ± 1 T (26.5% Fe; 83 K) (Daniels *et al* 1984), 30.5 T (24.5 at.% Fe; 4.3 K), 29.7 T (26.7% Fe; 4.3 K) (Palaith *et al* 1969), 28.0 ± 0.5 T (23.7 at.% Fe; 77 K), 27.5 ± 0.5 T (28.0 at.% Fe; 77 K) (Vinokurova *et al* 1969). Moreover, extrapolated values of the IS for the same local environment as in Pt_3Fe are 0.432 ± 0.027 mm s^{-1} (4.3 K), 0.365 ± 0.027 mm s^{-1} (77 K), 0.3199 ± 0.0075 mm s^{-1} (room temperature) which should be compared with 0.444 ± 0.004 mm s^{-1} (83 K) (Daniels *et al* 1984), 0.45 ± 0.03 mm s^{-1} (Vinokurova *et al* 1969) and 0.31 ± 0.01 mm s^{-1} (300 K) (Palaith *et al* 1969).

The intensity of the central peak, described at higher temperatures either by the wide Lorentzian line or by the low-field component of the HMFD, increases continuously with increasing temperature, and its IS becomes eventually the same as the IS of the Zeeman sextets. However, at low temperatures the IS of this line is systematically smaller by about 0.1 mm s^{-1} than the IS of the Zeeman sextets (figure 6(*a*)) for both samples, irrespective of their different degrees of order and different contents of the paramagnetic-like line. Hence one can conclude that the central line at low temperatures is caused by some kind of structural defect. Daniels *et al* (1984) showed that in Pt_3Fe an Fe atom located in the first coordination shell decreases the IS by about 0.034–0.092 mm s^{-1}. As the presence of an extra Fe atom should not lead to a very different shift in the IS than the presence of a Mn atom would, one could speculate that iron nuclei located in APBs should exhibit spectra with a lower IS than nuclei in the undisturbed positions do.

It has been reported that a 3d atom located at a platinum site in Pt_3Fe or Pt_3Mn changes the direction of the magnetic moment (Bacon and Crangle 1963, Menzinger *et al* 1972). Furthermore, from our preliminary measurements on $Pt_3Mn_xFe_{1-x}$ alloys with higher Fe contents, to be published in due time, it turns out that a relatively small change in the Fe-to-Mn ratio causes fairly drastic distortions of the Mössbauer spectra. Hence, it seems most probable that iron atoms located in APBs, usually having one Mn atom in the first coordination shells, will be responsible for the low-field component in the MHFD.

4.3. High-temperature behaviour

High-temperature measurements on slightly disordered $Pt_3Mn_{0.9}Fe_{0.1}$ (sample I) have shown that the shape of Mössbauer spectra could well be explained by the presence of relaxation phenomena (Szymański and Dobrzyński 1990). The results described here confirm this hypothesis. Together with the increase in the intensity of the paramagnetic-like line, other phenomena are observed, namely broadening of spectral lines with increasing temperature, changes in the intensities of sextets, and merging of the IS of the central line with the IS for the Zeeman sextets. All these features are also detected for sample II. The possibility that the samples are composed of two different components—a magnetic and a paramagnetic component—is most unlikely, as the relative intensity of the magnetic component varies with temperature. It is also not expected that the aforementioned phenomena are due to rearrangement of atoms because such a process should not occur in the temperature range covered by our experiment.

However, if relaxation occurs in the samples, the collapse of the Mössbauer spectra at higher temperatures should not be interpreted in terms of a MHFD. Hence, the commonly used interpretation of the data in terms of $P(H)$ (figure 2) is at higher temperatures physically meaningless.

The relaxation effects can originate from the influence of planar structural defects on the magnetic structure. Indeed, the APBs divide every powder grain into smaller subvolumes. For the reasons discussed below, these subvolumes behave like superparamagnetic particles.

When the slip-induced APB appears, it introduces in its vicinity a large disturbance of the magnetization distribution. Firstly, as already mentioned, the 3d atom becomes a nearest neighbour of another Fe or Mn atom. This in turn can modify the values of the magnetic moments of both neighbouring 3d atoms. In addition, the exchange interactions of the 3d atom in question with its surrounding are modified, too. Here it is expected that Fe–Fe, Fe–Mn and Mn–Mn exchange interactions can differ in both the values and the signs, which must result in a situation typical for frustrated systems. The change in the local magnetization can heavily disturb the magnetization distribution of platinum atoms as well. Secondly, because of the well known properties of platinum, the disturbance can extend far from the origin, thus modifying the magnetic moments of 3d atoms not in direct contact with the APB. Therefore, when the crystal is divided by APBs into subvolumes, the magnetization distribution in the vicinity of APBs must vary from place to place. In particular, it is expected that the regions separating the subvolumes, which preserved the ferromagnetic order, are frustrated to a large extent. The effective interaction between the subvolumes may therefore be weak.

There is another reason which can lead to the effective weakening of the interaction between the subvolumes. In the APB the pairs of 3d atoms are oriented along the direction dependent on the slip vector of the APB (Chin *et al* 1967). There are few such directions possible for a given plane containing APBs. The oriented pairs in the APB plane should

lead to anisotropic interactions of the magnetization within the subvolume with the few APBs creating this subvolume. The subvolume's magnetization can thus assume many equivalent positions.

Both effects described above lead to weakening of the effective interaction between the subvolumes. When the temperature increases, the effective anisotropy energy of the subvolume becomes comparable with the thermal energy and relaxation effects will occur.

In this picture it is clear why at low temperatures, when the relaxation effects are frozen, the Mössbuaer spectra and MHFD are similar for both samples. When the temperature increases, the relaxation effect occurs first in sample I, which contains a higher density of APBs.

If the paramagnetic-like line present at low temperatures is due to iron atoms located in the APBs, the density of dislocations can be estimated. In the case of the homogeneous distribution of dislocations in which the average distance between a pair of dislocations is equal to $1/\sqrt{\rho}$ (Ikeda and Takahashi 1984), the dislocation density ρ is of the order of n^2/α^2. Here, α is the lattice parameter and n denotes the fraction of Fe atoms located in the APB. If n is assumed to have the same order of magnitude as the relative content of the central line in the Mössbauer spectrum at low temperatures, i.e. 4–10% and the lattice constant is $\alpha = 3.89$ Å (Pt_3Mn) (Pickart and Nathans 1962), one obtains $\rho = 10^{12}$–10^{13} cm^{-2} which corresponds to an average distance between dislocations of 30–100 Å. This distance can be considered as the average diameter of the subvolumes into which the samples are divided by the APBs. In $Pt_3Mn_xFe_{1-x}$ rolled at room temperature the dislocation density was estimated by Shreiner *et al* (1985) to be 10^{10}–10^{11} cm^{-2} and in the work of Ikeda and Takahashi (1984) the theoretical value of 5.5×10^{14} cm^{-2} was estimated to be necessary for inducing a transition from antiferromagnetism to ferromagnetism in Pt_3Fe. The region of ρ-values obtained from the central line intensity in the Mössbauer spectra lies in between these values. Furthermore, in the case of weakly interacting ferromagnetic particles of such a size, superparamagnetic behaviour is frequently observed. Therefore, relaxation effects in such a system seem rather natural.

5. Conclusions

During cold-work treatment of $Pt_3Mn_{0.9}Fe_{0.1}$ a large number of structural defects are introduced into the material. In the annealing process the $L1_2$ superstructure is formed first and then the defects are annealed. The presence of various Zeeman sextets is due to different local environments caused by substitution of Mn by Fe in the second coordination shell. Because the dislocations and ABPs are not totally removed by the thermal treatment, the bulk material is divided into weakly interacting volumes. When the temperature is raised and the effective anisotropy of subvolumes lowered, a relaxation process occurs and shows up primarily in an enhancement of the central peak in the Mössbauer spectrum.

Acknowledgments

The authors wish to thank Professor G Le Caer for providing the computer program and Professor S Morp for helpful discussions at the early stage of this work. The work was sponsored by the Jagiellonian University, Cracow through the CPBP 01.09 program.

References

Bacon G E and Crangle J 1963 *Proc. R. Soc.* **272** 387–405
Chin G Y, Nesbitt E A and Wernick J H 1967 *J. Appl. Phys.* **38** 2623–9
Crangle J 1959 *J. Physique Radium* **20** 435–7
Daniels J M, Julian S R, Lam H Y and Li P L 1984 *Can. J. Phys.* **63** 409–16
Elkholy H and Nagy E 1962 *J. Phys. Chem. Solids* **23** 1613–9
Ikeda K and Takahashi S 1984 *J. Appl. Phys.* **55** 3726–31
Le Caer G and Dubois J M 1979 *J. Phys. E: Sci. Instrum.* **12** 1083–90
Menzinger F, Sacchetti F and Romanazzo M 1972 *Phys. Rev.* B **5** 3778–82
Palaith D, Kimball C W, Preston R S and Crangle J 1969 *Phys. Rev.* **178** 795–9
Pickart S J and Nathans R 1962 *J. Appl. Phys.* **33** 1336–8
Segnan R 1967 *Phys. Rev.* **160** 404–8
Shreiner W H, Stamm W and Wassermann E F 1985 *J. Phys. F: Met. Phys.* **15** 2009–23
Sidorov C K and Dubinin S F 1967 *Fiz. Metall. Metalloved.* **24** 859–67
Stamm W and Wassermann E F 1986 *J. Magn. Magn. Mater.* **54–7** 161–2
Szymański K and Dobrzyński L 1990 *J. Magn. Magn. Mater.* **83** 181–2
Vinokurova L I, Nikolayev I N, Mel'nikov Ye V, Adis'yevich I K, Reiutov Yu B 1969 *Fiz. Metall. Metalloved.* **28** 1098–102
Vokhmyanin A P, Kelarev V V, Pirogov A N and Sidorov S K 1980 *Fiz. Metall. Metalloved.* **46** 67–74